

Accurate Measurements of the Brightness of the White-Light Corona at the Total Solar Eclipses on 1 August 2008 and 22 July 2009

Yoichiro Hanaoka · Yoshihiro Kikuta · Jun Nakazawa ·
Kouji Ohnishi · Kazuo Shiota

Received: 30 December 2011 / Accepted: 25 March 2012 / Published online: 19 April 2012
© Springer Science+Business Media B.V. 2012

Abstract We measured the brightness of the white light corona at the total solar eclipses on 1 August 2008 and 22 July 2009, when solar activity was at its lowest in one hundred years. After careful calibration, the brightness of the corona in both eclipses was evaluated to be approximately 0.4×10^{-6} of the total brightness of the Sun, which is the lowest level ever observed. Furthermore, the total brightness of the K + F-corona beyond $3R_{\odot}$ in both eclipses is lower than some of the previous measurements of the brightness of the F-corona only. Our accurate measurements of the coronal brightness provide not only the K-corona brightness during a period of very low solar activity but also a reliable upper limit of the brightness of the F-corona.

Keywords Corona · Photometry · White-light

1. Introduction

The solar minimum between cycles 23 and 24, which occurred at the end of 2008, showed the activity level to be significantly lower than that of the other recent minima. Two total solar eclipses occurred around this minimum on 1 August 2008 and on 22 July 2009. Some

Y. Hanaoka (✉)

National Astronomical Observatory of Japan, Mitaka, Tokyo, Japan
e-mail: hanaoka@solar.mtk.nao.ac.jp

Y. Kikuta

Yamanashi Prefectural Science Center, Kofu, Yamanashi, Japan

J. Nakazawa

Yamanashi Cement Company, Kofu, Yamanashi, Japan

K. Ohnishi

Nagano National College of Technology, Nagano, Japan

K. Shiota

Solar Eclipse Information Center, Odawara, Kanagawa, Japan

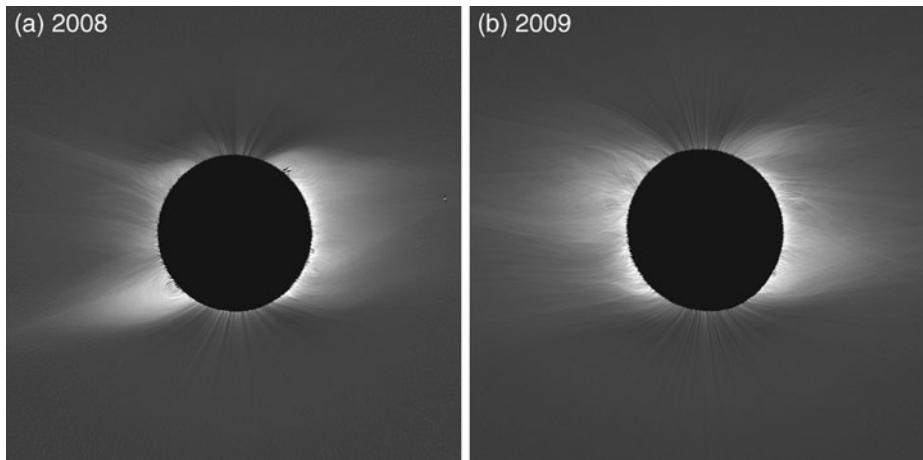


Figure 1 Stacked images of the white-light corona taken in (a) the 1 August 2008 eclipse and (b) the 22 July 2009 eclipse. To show the fine structures in the corona clearly, radial brightness decrease is suppressed, and structures of the coronal streamers are enhanced. The solar north is to the top.

studies putting stress on the structures of the deep minimum corona seen in the white-light corona and the E-corona at these eclipses have already published (Pasachoff *et al.*, 2009, 2011; Habbal *et al.*, 2010; Voulgaris *et al.*, 2010). On the other hand, these eclipses were good chances to measure the coronal absolute brightness during such a deep minimum. The brightness of the corona is known to show significant dependence on the solar activity (*e.g.* Rušin, 2000).

To ensure obtaining data of total eclipses under good weather conditions, it is helpful to dispatch several expeditions along the eclipse belt. Nowadays many commercial eclipse tours are offered. The participants on such tours often have small telescopes and digital single-lens reflex (DSLR) cameras. These are suitable instruments to deploy observers widely because such instruments can be operated as “stand-alone” devices, and at the same time they are high performance imaging instruments for the white light corona as demonstrated by fantastic images processed by M. Druckmüller (see *e.g.* Druckmüller, Rušin, and Minarovjeh, 2006).

In the 2009 eclipse, the Moon’s umbral shadow passed from India to the Pacific Ocean, and the observing conditions were very good – the Sun passed near the zenith, and the duration of the totality was long. Therefore, as well as sending our own professional expeditions, we collaborated with participants of commercial eclipse tours to observe this eclipse. Unfortunately the weather conditions were not very good as a whole, but some observers on commercial tour ships succeeded in obtaining high-quality data. In the 2008 eclipse, the Moon’s umbral shadow mainly passed through Russia and China. Though the observing conditions were not very good, namely the altitude of the Sun was low and the duration of the totality was short, we carried out an imaging observation in China, and successfully obtained data for photometry under fairly good weather conditions. Eventually we obtained well-calibrated brightness data of the white-light corona at the 2008 and 2009 eclipses, when the deep solar minimum occurred in between. The obtained images of the white light corona are shown in Figure 1. The observations and the data reduction are described in Sections 2 and 3, respectively. In Section 4, we present results and discussion on the measured total brightness of the K + F-corona, on which we concentrate in this paper. The calibrated images of the white-light corona show the distribution of the electron column densities in the

fine structures of the corona during the deep minimum, and this will be discussed in another paper.

2. Observations

The observations are listed in Table 1. All observations were done with small telescopes and DSLR cameras, and calibration data were taken as well as images of the corona. We have the data of the 2009 eclipse obtained by four observers YK, JN, KO, and KS as shown in Table 1. Because our purpose in this paper is to measure the brightness of the corona accurately, we checked calibration images, particularly placing stress on the reliability and consistency of the transmission of the ND filters used to take images of the solar disk. Such cross-checking of the calibration data was made possible by gathering observational data taken by various observers, and it significantly contributed to the reliability of the photometric results. In other words, we might overlook a photometric error if we were to use data from only a single observation. We judged that the data set by KO give the most consistent photometric results, and hereafter we present the analysis of this data set for the 2009 eclipse.

On the other hand, we have only one data set for the 2008 eclipse. However, we were able to confirm the consistency of the calibration data, comparing the effective throughput of the ND filter used in 2008 and that in 2009 by taking solar images with a common optics after the eclipses. Therefore, we included it in our analysis and compare the results with the 2009 eclipse.

3. Data Reduction to Obtain Calibrated Coronal Images with a High Dynamic Range

A single raw image taken with a DSLR camera contains data of three color channels, namely red (R: around 600 nm), green (G: around 530 nm), and blue (B: around 460 nm). Firstly we divided raw images into three color channels, and then carried out the following reduction procedures.

3.1. Stacking Images – The Case of the 2009 Eclipse

The purpose of the data reduction is to obtain calibrated coronal data with a high dynamic range and a high signal-to-noise ratio. To cover the wide dynamic range of the coronal brightness distribution, many coronal images were taken with a wide range of exposure times as shown in Table 1. The large number of images also contributed to increasing the signal to noise ratio. Therefore, stacking many images achieved a high dynamic range and a high signal-to-noise ratio. Each image records the amount of light coming into the camera during the exposure time. The exposure time of DSLR cameras might slightly differ from the nominal ones, and then we measured correct exposure times using the flat-field images taken with various exposure times. The images were normalized by the correct exposure times. Next, we calculated shifts and rotations between the images. The images were taken on vessels; the field of view moved with the pitching and the rolling of the vessel. To align the images, we compared a part of the coronal streamer structure and three stars on each image, of which the identifier numbers in the Tycho-2 catalogue (Høg *et al.*, 2000) are 1388 01791 1, 1384 02038 1, and 1384 02046 1. Figure 2 shows the positions of the field of view of the images in the 2009 eclipse taken by KO with respect to the corona. The positions of the stars are also used to determine the scale (arcsec per pixel) and the orientation (the direction of the celestial north) of the images.

Table 1 Parameters of the observations of the 2008 and 2009 eclipses.

Date	1 August 2008	22 July 2009			
Observer	Y. Hanaoka (YH)	Y. Kikuta (YK)	J. Nakazawa (JN)	K. Ohnishi (KO)	K. Shiota (KS)
Observation site	Jinta, Gansu, China	Near Kita-Iwojima (Pacific Venus Vessel)	Near Kita-Iwojima (Pacific Venus Vessel)	Near Kita-Iwojima (Fujimaru Vessel)	Near Kita-Iwojima (Pacific Venus Vessel)
Geographic coordinate	40N99E	26N142E			
Duration of the totality	1 m 36 s	6 m 39 s			
Altitude of the Sun	14°	84°			
Telescope specs	Refractor D60 mm f350 mm	Refractor D80 mm f640 mm	Reflector D160 mm f1280 mm	Refractor D101 mm f540 mm	Refractor D106 mm f530 mm
Camera	Nikon D300	Canon EOS5DmkII	Canon EOS5DmkII	CanonEOS5DmkII	Canon EOS5DmkII
Data format	4320 × 2868, 14 bits	5634 × 3753, 14 bits	5634 × 3753, 14 bits	5634 × 3753, 14 bits	3866 × 2574, 16 bits*
FOV (diagonal)	4.6°	3.9°	1.9°	4.6°	4.7°
Range of exposure time	1/8–1/500 s	1/2–1/8000 s	1/15–1/2000 s	1/5–1/2000 s	1/15–1/8000 s
Number of images of the corona	22	243	89	202	160

* A kind of lossy data compression applied.

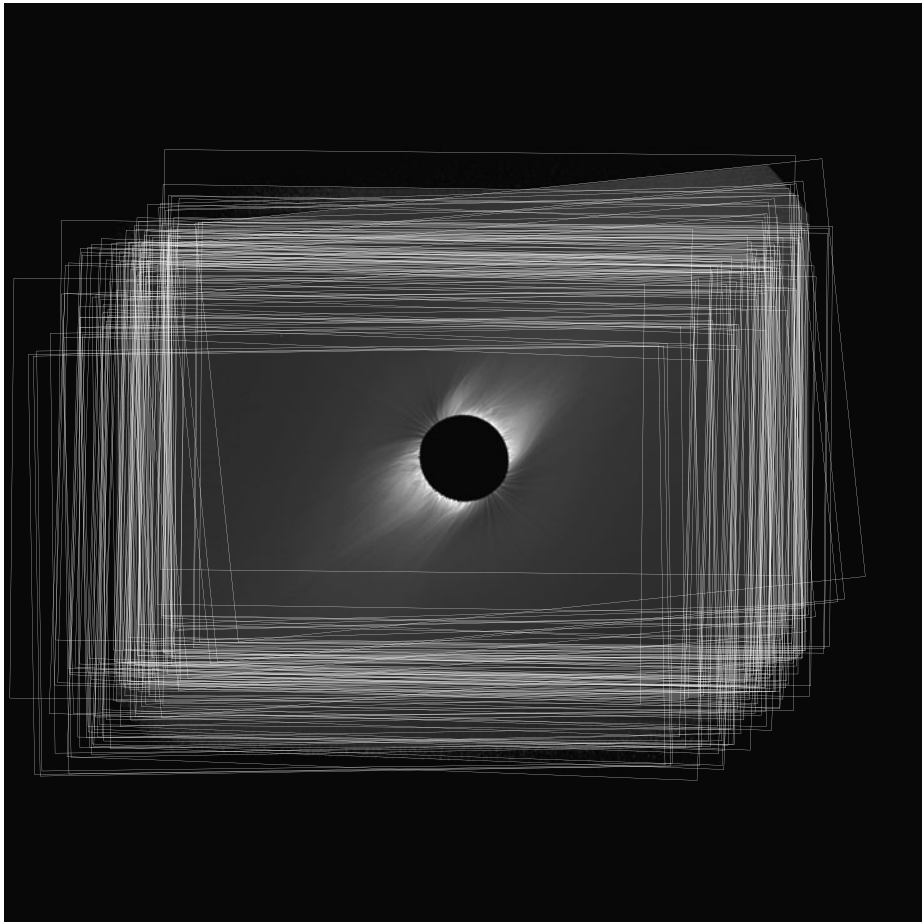
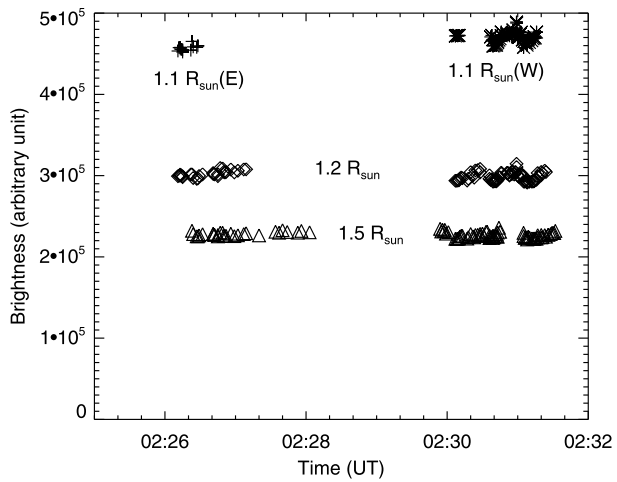


Figure 2 Positions of the field of view of 202 images taken by KO during the totality of the 2009 eclipse, with respect to the solar corona.

After the coalignment of the images based on the evaluated shifts and rotations, we can stack up the images. However, before that, we need to check if the transparency of the air was constant during the totality. We measured the variation of the brightness of the corona during the totality in the KO data set. In Figure 3, we show the average, exposure-corrected coronal brightness at heights of 1.1, 1.2, and 1.5 R_{\odot} for each image. The circle of 1.1 R_{\odot} is partially covered by the Moon during the totality. Therefore, the average brightness values of the eastern and the western arcs were calculated for the former and latter halves of the totality separately. If the image was overexposed or underexposed at any height, the brightness was not plotted. Figure 3 shows that the brightness change was within $\pm 3\%$, and we can conclude that the sky condition was stable throughout the totality. Therefore, the images can be safely stacked. For each image, we set the unity weight for the properly exposed portions, zero weight for over-exposed and under-exposed portions, and for portions between properly exposed area and over/under-exposed area we set small weight, and stacked them. We calculated weighted mean for each pixel, and eventually we obtained a coronal image with a high dynamic range and a high signal-to-noise ratio, as shown in Figure 1b.

Figure 3 Average brightness of the corona at the heights of 1.1, 1.2, and 1.5 R_{\odot} measured on 202 exposure-corrected images taken by KO during the totality of the 2009 eclipse.



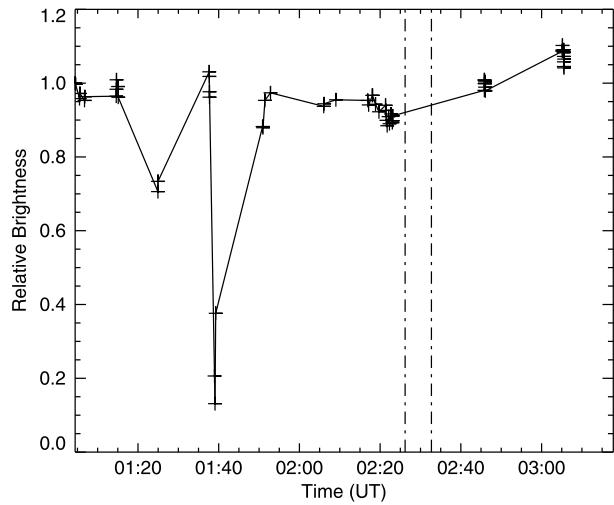
3.2. Brightness Calibration – The Case of the 2009 Eclipse

The brightness on the obtained coronal image needs to be calibrated to evaluate the brightness relative to the solar disk. We have images of the solar disk taken with the same instruments (with ND filters) as those for the totality from around the first contact to after the third contact. Firstly we checked the stability of the measured, exposure-corrected brightness of the solar disk. We picked up an image taken before the first contact as the reference, and calculated the relative brightness of the partially eclipsed Sun, comparing the brightness of the residual disk portion of the eclipsed Sun and the corresponding part of the reference image. Figure 4 shows the variation of the relative brightness of the disk in the KO data set. Except for some sudden decreases, the brightness was mostly kept within $\pm 5\%$ of the reference brightness. The altitude of the Sun was 66° or higher, so the atmospheric extinction can be ignored. Therefore, the result means that most of the partial eclipse images were taken under the clear sky, except occasional cloud passages. It is safely assumed that during the totality the condition of the sky was similar to the partial eclipse phase just before and just after the totality. Based on the results shown in Figure 4, interpolating the disk brightness values before and after the totality, which show a difference of about 10% , we defined the brightness of the solar disk as being 0.98 of the reference image, and we calibrated the brightness of the corona referring to this disk brightness. The uncertainty of the disk brightness leads to the calibration error of $\pm 5\%$.

The coronal brightness with respect to the disk brightness can be calculated with the transmission of the ND filter used to take images of the partial eclipse. Some ‘AstroSolar’ filters fabricated by Baader Planetarium and other neutral density filters were used for the observations, but actually, the transmission is not neutral but depends on the wavelength. In such a case, the wavelength distributions of the detected light by the CCD for the corona and for the disk (with ND filters) differ. The effective transmission for each of R, G, and B channels of a ND filter is calculated as follows. We can write the signal read from the CCD without the ND filter as

$$I_{\text{nofilter}}^C = \int D^C(\lambda) S(\lambda) d\lambda, \tag{1}$$

Figure 4 Variation of the relative brightness of the solar disk from the first contact to after the third contact of the 2009 eclipse measured on the images taken by KO.



and with the ND filter as

$$I_{\text{filter}}^C = \int D^C(\lambda) F(\lambda) S(\lambda) d\lambda, \tag{2}$$

where C is any color of R, G, and B, and $D^C(\lambda)$, $F(\lambda)$, and $S(\lambda)$ are spectral characteristics of detector sensitivity, filter transmission, and solar light. For $D^C(\lambda)$, we adopted the measured values by Sigernes *et al.* (2009) for Nikon D300 and those by C. Buil (<http://astrosurf.com/buil/index.htm>) for Canon EOS5DmkII, and we measured $F(\lambda)$ mainly with a spectrophotometer SolidSpec 3700 (Shimadzu Corp.). For the values $S(\lambda)$, we adopted standard and reference spectra distributed by National Renewable Energy Laboratory prepared by ASTM (formerly the American Society for Testing and Materials). The difference between the spectral characteristics of the light from the solar disk and that from the corona due to the F-corona was ignored. We calculated I_{nofilter}^C and I_{filter}^C , and the ratio $I_{\text{nofilter}}^C/I_{\text{filter}}^C$ is the effective transmission of the ND filter.

3.3. The 1 August 2008 Eclipse

We carried out reductions similar to those described above for the data of the 2008 eclipse. However, the eclipse occurred at a low altitude (14°), and therefore, transparency of the air decreased rapidly with the progress of the eclipse. Since the transmission in the B channel was low and showed particularly rapid change, we analyzed the R and G channels only. In addition, thin cloud passages affected the transparency. We calibrated the coronal images using the partial eclipse images just before and just after the totality, and the uncertainty of the stability of the disk brightness is $\pm 10\%$.

4. Results

As shown above, we obtained high signal-to-noise ratio images of the white-light corona with a wide dynamic range based on the composite of many pictures taken with various exposure times. Here we discuss total brightness of the corona and average radial brightness distributions.

Table 2 Total coronal brightness and sky brightness at the 2008 and 2009 eclipses. Total brightness is shown in units of L_{\odot} , the total brightness of the Sun, and the sky brightness is shown in units of B_{\odot} , the average surface brightness of the Sun.

	2008 Total (1.03–4 R_{\odot}) $10^{-6}L_{\odot}$	2008 Sky $10^{-8}B_{\odot}$	2008 Total, sky-removed $10^{-6}L_{\odot}$	2009 KO Total (1.03–6 R_{\odot}) $10^{-6}L_{\odot}$	2009 KO Sky $10^{-8}B_{\odot}$	2009 KO Total, Sky-removed $10^{-6}L_{\odot}$
R	0.425	0.125	0.406	0.405	0.022	0.398
G	0.456	0.182	0.428	0.399	0.032	0.388
B	–	–	–	0.401	0.050	0.383

4.1. Total Brightness of the Corona

The variation of the total brightness of the corona shows a good agreement with the cycle variation of the solar activity; see *e.g.* Rušin (2000), where the total brightness values of the white light corona (1.03–6.00 R_{\odot}) measured at various total eclipses over the past one hundred years are compiled, and the total brightness has varied mostly in the range of $0.5–1.4 \times 10^{-6}$ in units of the total brightness of the Sun.

We calculated the total brightness of the white light corona (K + F-corona) for the 2008 eclipse and the 2009 eclipse (KO data), and the results are shown in Table 2. Total brightness of 1.03–6 R_{\odot} in the 2009 eclipse including the sky brightness is around $0.4 \times 10^{-6}L_{\odot}$, where L_{\odot} is the total brightness of the Sun. The sky brightness values discussed in the next subsection are also shown in Table 2, as well as the total brightness values without the sky brightness. The estimated brightness is somewhat lower than $0.40 \times 10^{-6}L_{\odot}$. This value is lower than $0.48 \times 10^{-6}L_{\odot}$ recorded in 1954 (near a solar minimum), which is the lowest value in the compilation by Rušin (2000) except a suspect value recorded at one of the eclipses in 1968.

Actually, the radius of the Moon was 1.06 R_{\odot} at the 2009 eclipse, and therefore, a part of the annulus of 1.03–1.06 R_{\odot} was always covered by the Moon, and part of coronal brightness was not counted in the values in Table 2. However, based on the coronal brightness in the uncovered part of the annulus of 1.03–1.06 R_{\odot} , we can estimate that the contribution of the covered part is a few per cent of the total brightness. Therefore, even if we take this error and the uncertainties in the absolute calibration mentioned in Section 3 into account, we can conclude that the total brightness of the corona in 2009 was the lowest level ever observed.

In Table 2, we show the total brightness in the R and G channels in 2008 (1.03–4 R_{\odot}) as well, both of the brightness values including and excluding the sky. Again it shows lower values than that in 1954. Therefore, even if we take into account that the values in 2008 may include $\pm 10\%$ error (and only $<4R_{\odot}$ was integrated), we can conclude that the coronal brightness in 2008–2009, between which the deep minimum occurred, significantly dropped similarly to the solar activity. Although these eclipses were good chances to measure the coronal brightness at the deep minimum, there are no other results published except for a report by Skomorovsky *et al.* (2012) for the 2008 eclipse. However, they took a model brightness distribution (Koutchmy and Lamy, 1985) as a reference for the photometric analysis of the K + F-corona, and therefore, their results cannot be considered as absolute photometry in a real sense.

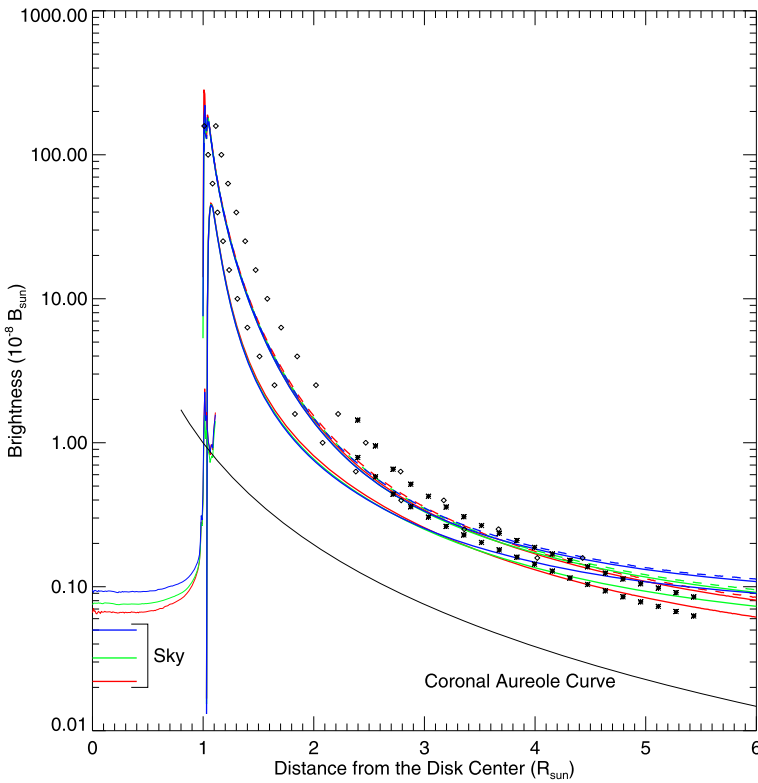


Figure 5 Polar (lower thick solid curves) and equatorial (upper thick solid curves) radial distributions of the K + F-coronal brightness of the 2009 eclipse for the R, G, and B channels, which are shown by red, green, and blue curves, respectively. At each distance from the disk center, brightness values in sectors within $\pm 22.5^\circ$ around the solar north, south, east, and west are averaged. The average within $\pm 2^\circ$ around the east and west equators are also shown (thick dashed curves). Brightness distributions in the R, G, and B channels in the Moon’s image are shown by thin solid curves. The brightness of the sky is not removed from the above curves, but the estimated sky brightness levels for the R, G, and B channels are also shown. The estimated brightness profile of the coronal aureole is shown by a solid black curve. Examples of the previously published results of the measurements of polar and equatorial K + F-coronal brightness near the solar minimum are also shown; diamonds are results by Saito (1970), and stars are results by Morgan and Habbal (2007).

4.2. Radial Brightness Distributions

4.2.1. Radial Brightness Distributions with and Without Sky Background and Coronal Aureole

We calculated mean polar and equatorial radial brightness distributions of the K + F-corona of the 2009 eclipse, averaging brightness at each radius in sectors within $\pm 22.5^\circ$ around the solar north and the solar south, and the solar east and the solar west. The results for each of the R, G, and B channels are shown in Figure 5 with thick, solid red, green, and blue curves. In addition, we calculated the average within $\pm 2^\circ$ around the east and west equators, which shows the sharp peak of the brightness at the equator (dashed curves in Figure 5). Figure 5 also shows the polar and the equatorial curves of the K + F-corona by Saito (1970; mostly based on total eclipse data) and by Morgan and Habbal (2007; based on C2 coronagraph

measurements by Large Angle and Spectrometric CORonagraph [LASCO] of *Solar and Heliospheric Observatory* [SOHO]), which show the typical values of the minimum corona among the previously published results. Although the brightness shown in Figure 5 includes the brightness of the sky and the coronal aureole, Figure 5 shows that our results within $4 R_{\odot}$ are lower than previously published ones. This fact is consistent with the low total brightness described in Section 4.1.

It is necessary to remove the sky background and the coronal aureole to carry out more accurate comparison. While the sky background is approximately constant in the field of view, the brightness distribution of the coronal aureole, which is the scattered light mainly from the bright inner corona, depends on the sky condition and the instrumental scattered light. A ‘diamond ring’ picture in the data set by KO shows that the scattered light from the small crescent portion of the solar disk decreases in proportion to $r^{-2.4}$, where r is the distance from the source in units of solar radius. The power law indices of the coronal aureole derived by the previous analyses rather scatter, but Lebecq, Koutchmy, and Stellmacher (1985) gave -2.5 , which is similar to our value. A curve, $r^{-2.4}$, is shown in Figure 5 to show how the coronal aureole looks. However, it is difficult to measure the absolute level of the coronal aureole as well as the sky brightness directly from our data, so we estimated them on the following assumptions.

- The ratio among the brightness values of the sky in the R, G, and B channels during the totality is approximately the same as those of the sky out of the eclipse (namely, usual blue sky) in the calibration images.
- The brightness of the Moon measured during the totality (they are also shown in Figure 5) corresponds to the sum of the earthshine, coronal aureole (both are approximately white), and the sky brightness. Therefore, the differences among the Moon’s brightness values of the R, G, and B channels approximately correspond to the differences among the three channels of the sky brightness.
- The slope of the radial brightness variation after the removal of the sky brightness and the coronal aureole is not much different from those of the various former results.

Flattening of the measured radial profiles in the outer corona in Figure 5 signifies the definite contribution of the sky brightness. The estimated sky brightness values are shown in Figure 5, and the results of the subtraction of the sky background from the measured values are shown in Figure 6. The brightness of the Moon in Figure 6 is about $0.042 \times 10^{-8} B_{\odot}$ (B_{\odot} is the average brightness of the solar disk). The brightness of the earthshine is known to be about $0.03 \times 10^{-8} B_{\odot}$ (see *e.g.* Dürst, 1982), and therefore, the remaining coronal aureole in the Moon, surrounded by the bright inner corona, is so small that the contribution from the coronal aureole is negligible in the outer corona. Consequently we can consider that Figure 6 shows the brightness of the K + F-corona in 2009. Actually our sky brightness values, $0.022\text{--}0.050 \times 10^{-8} B_{\odot}$, are smaller than those by the previous measurements (*e.g.*, $0.22 \times 10^{-8} B_{\odot}$ by Lebecq, Koutchmy, and Stellmacher (1985) in green, and $0.066 \times 10^{-8} B_{\odot}$ by Dürst (1982) at 600 nm). Note that the possible underestimation of the sky brightness and ignorance of the coronal aureole cause possible overestimation of the brightness of the K + F-corona.

4.2.2. Comparison with the Previously Measured F-corona

An interesting result was obtained from the comparison between the observed brightness of the K + F-corona in 2009, and the formerly measured brightness of the F-corona. In Figure 6, polar and equatorial brightness values of the F-corona by Morgan and Habbal

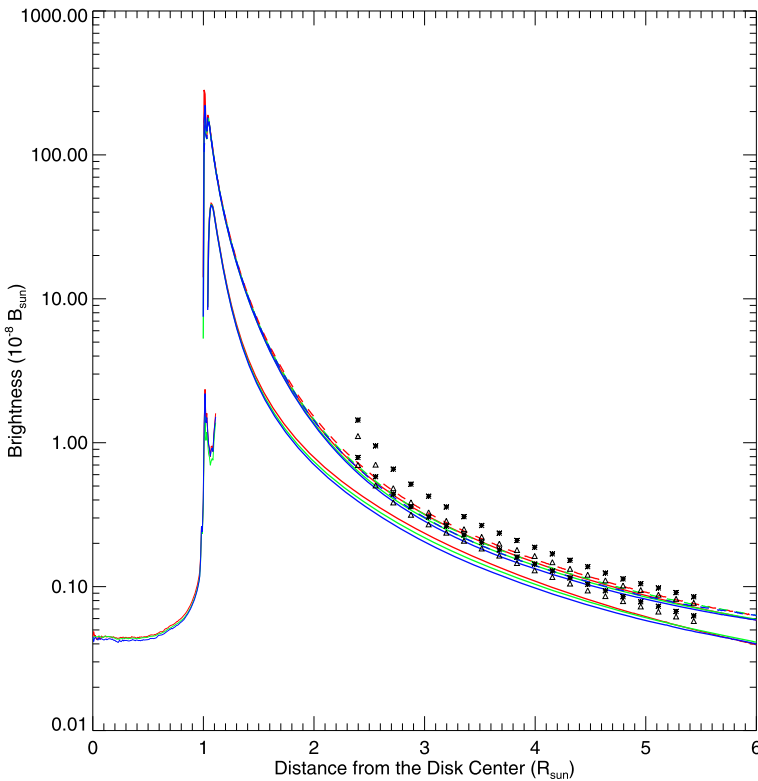


Figure 6 Polar and equatorial radial distributions of the K + F-coronal brightness of the 2009 eclipse after the removal of the sky brightness. Red, green, and blue curves have the same meanings as in Figure 5. The measurements of polar and equatorial K + F-coronal brightness (stars) and F-corona brightness (triangles) by Morgan and Habbal (2007) are also shown.

(2007) measured in the wavelength range 540–640 nm and average $\pm 2^\circ$ around the north, south, east, and west are shown by triangles, along with their K + F-corona brightness values shown by stars. It is clear that the polar K + F-corona brightness values observed in 2009 are lower than the F-corona brightness obtained by Morgan and Habbal (2007). To show that fact more clearly, a comparison between the results by Morgan and Habbal (2007) and our measurements in 2009 for the R channel, which is approximately the same wavelength range as that of Morgan and Habbal (2007), is shown in Figure 7. Their results (triangles) within $3 R_\odot$ are possibly too high due to some instrumental effect. Even if we ignore the data inside $3 R_\odot$, our K + F values (gray curves) show substantially smaller brightness than the F-corona values of Morgan and Habbal (2007) in the polar regions. For the equatorial regions, our K + F values shown by a dashed gray curve, which are an average of $\pm 2^\circ$, are comparable to their results for the F-corona. They showed various previously published results for the F-corona in their Figure 3. Although some other measurements of the F-corona show good coincidence with their results, a measurement by Dürst (1982) around 600 nm gives lower brightness than others. His results for the F-corona are shown in Figure 7 with solid black curves, and they are lower than our results for the K + F-corona in the equator and comparable to ours in the pole. In addition, we showed model brightness distributions of the F-corona in the range of 400–600 nm by Koutchmy and Lamy (1985) with dotted

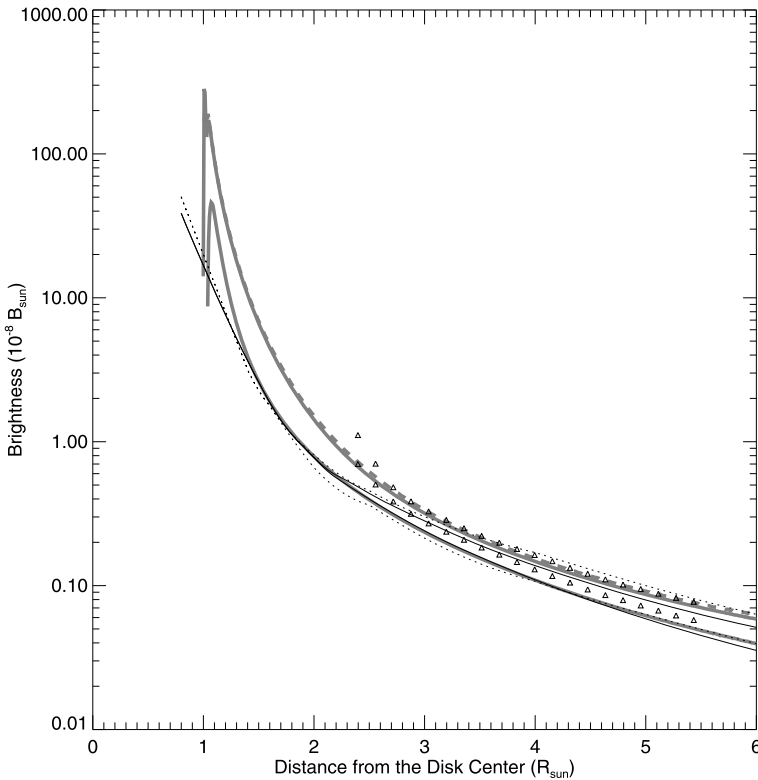


Figure 7 Polar and equatorial radial distributions of the K + F-coronal brightness of the 2009 eclipse in the R channel after the removal of the sky brightness. The red curves in Figure 6 are duplicated with gray curves in this figure. The measurements of polar and equatorial F-corona brightness by Morgan and Habbal (2007) are shown by triangles, those by Dürst (1982) are shown by solid black curves, and model brightness distributions of the F-corona by Koutchmy and Lamy (1985) are shown by dotted black curves.

black curves. Their model brightness at the pole is somewhat lower than ours and Dürst's (1982) within $4 R_{\odot}$, while their model shows a brightness higher than the measurements by Morgan and Habbal (2007) at the equator beyond $3 R_{\odot}$.

For the 2008 eclipse data, we estimated the coronal brightness without sky in a similar way. Figure 8 shows the comparison between the 2008 R and G channel data and the brightness of the F-corona by Morgan and Habbal (2007, triangles), Dürst (1982, solid black curves), and Koutchmy and Lamy (1985, dotted black curves). Our results for the polar K + F brightness are again lower than the results for the F-corona by Morgan and Habbal (2007) and similar to those by Dürst (1982). Furthermore, unlike the 2009 results, our equatorial brightness is somewhat lower than the results for the F-corona by Morgan and Habbal (2007), and beyond $3.5 R_{\odot}$, it is close to the F-corona brightness by Dürst (1982).

In Figure 9, we show tangential brightness distributions of the K + F corona of the 2008 (dashed curves) and the 2009 (solid curves) eclipses at various heights from the disk center. Although coronal streamers dominate except in small gaps at the north and south poles at low heights $< 2.0 R_{\odot}$ (Figure 9a), they converge around the equator at higher heights, and finally only narrow streamers remain around the equator (Figure 9b). In Figure 9b, we show the values obtained by Fainshtein, Tsivileva, and Kashapova (2010, plus signs), who pre-

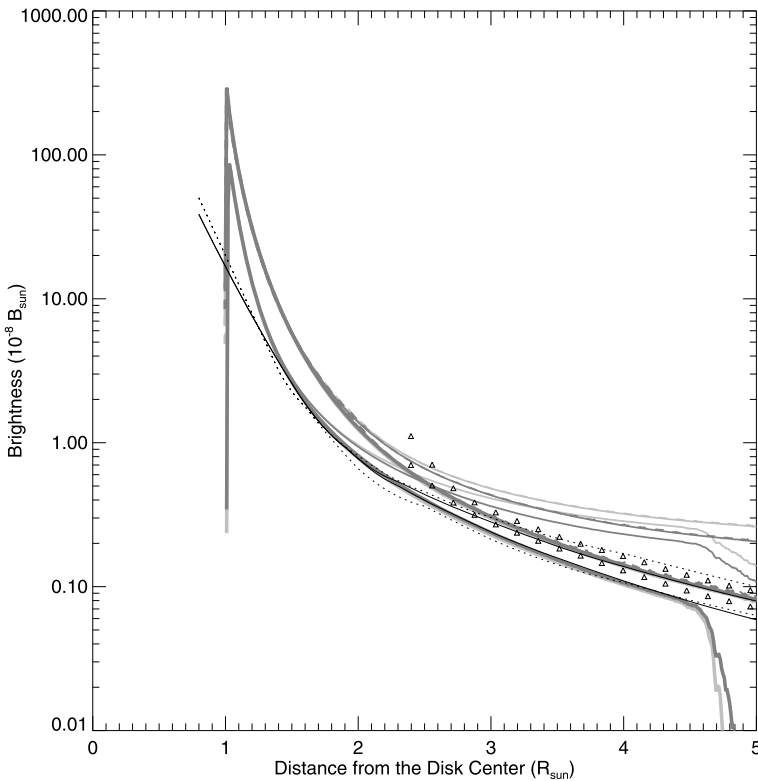


Figure 8 Polar (lower gray curves) and equatorial (upper gray curves) radial distributions of the total coronal brightness of the 2008 eclipse for the R and G channels, which are shown by dark gray and light gray curves, respectively. At each distance from the disk center, brightness values in sectors within $\pm 22.5^\circ$ around the solar north, south, east, and west are averaged. The averages within $\pm 2^\circ$ around the east and west equators are also shown (dashed curves). Profiles with and without sky are shown by thin and thick curves. The measurements of polar and equatorial F-corona brightness by Morgan and Habbal (2007) are shown by triangles, those by Dürst (1982) are shown by solid black curves, and model brightness distributions of the F-corona by Koutchmy and Lamy (1985) are shown by dotted black curves.

sented the latitudinal variation of the F-corona at heights of 2.5, 3.5, 4.5 R_\odot etc. based on the analysis of SOHO/LASCO C2 observations. They gave the results in 1997 and 2000, but we only plotted the results in 1997, near the solar minimum. Since they did not give the results for the western equator, we duplicated the brightness of the eastern equator at the position angle 270° (western equator). We also plotted the F-corona brightness by Morgan and Habbal (2007, triangles) and Dürst (1982, stars) for 2.5, 3.5, and 4.5 R_\odot . Since Dürst (1982) gave the average of the north and south poles and the eastern and the western equators, we plotted the same values for the north and south poles, and the eastern and western equators. We can confirm the relation between our K + F results and the previous F-corona measurements; the results from LASCO data (plus signs and triangles) are systematically higher than ours, particularly at the pole areas (note that at 2.5 R_\odot the LASCO results are possibly too high because of the instrumental effect).

For the polar areas, our K + F brightness in both 2008 and 2009 eclipses is smaller than the F-corona brightness by Morgan and Habbal (2007) and Fainshtein, Tsivileva, and Kashapova (2010) by 20 % or more. Although the calibration may include up to 10 %

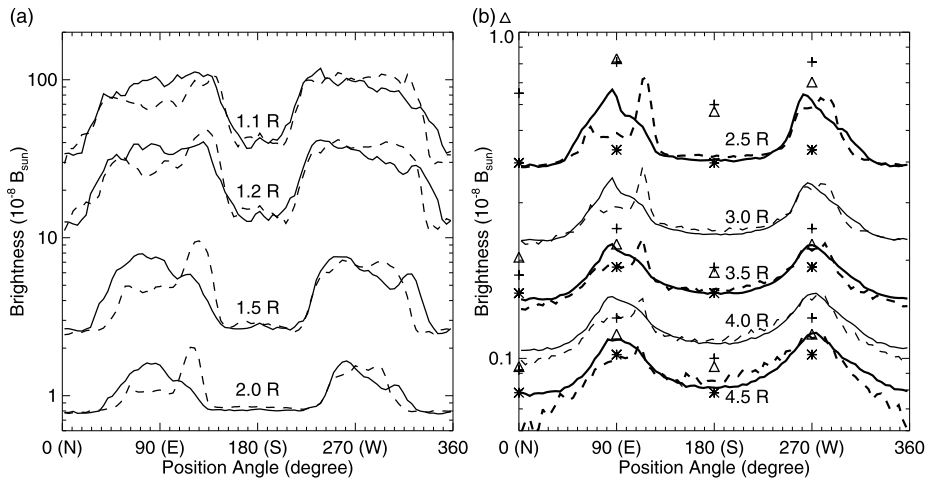


Figure 9 Tangential coronal brightness distributions in the 2008 (dashed curves) and the 2009 (solid curves) eclipses. (a) Radii of 1.1, 1.3, 1.5, and 2.0 R_{\odot} . (b) Radii of 2.5, 3.0, 3.5, 4.0, and 4.5 R_{\odot} . Brightness values of the F-corona measured by Morgan and Habbal (2007), by Fainshtein, Tsivileva, and Kashapova (2010), and by Dürst (1982) for radii 2.5, 3.5, and 4.5 R_{\odot} are also shown by triangles, plus signs, and stars. Our results for these radii are shown in thick curves. Since Fainshtein, Tsivileva, and Kashapova (2010) did not give the values for the west limb, the value of the east limb is duplicated at the west limb. Since Dürst (1982) gives the average of the north and south poles and that of the east and west equators, the same values are plotted for the north and south poles and for the east and west equators.

and 5 % errors for the 2008 and 2009 data, respectively, we can safely conclude that the brightness of the F-corona in both 2008 and 2009 is lower than typical brightness of the F-corona formerly published. In Figure 9, the results by Dürst (1982) give similar values in the polar areas and lower values at the equatorial areas. In the equatorial regions, we can find distinct coronal streamer structures, which means that there should be a certain contribution from the K-corona. Attention should be paid to the fact that at the eastern equator our results in 2008 are comparable to those of Dürst (1982). At the east limb in 2008, the bright streamer was located to the south (see also Figure 1b). Therefore, our result at 90° (E) is presumed to include only a small contribution from the K-corona. The polar region contains a small amount of K-corona and our results and those by Dürst (1982) are comparable. Therefore, the results for the F-corona by Dürst (1982) are considered to be consistent with our results for the K + F-corona.

The formerly measured brightness values of the F-corona in visible wavelengths show some scatter (see *e.g.* Morgan and Habbal, 2007). The reason for this scatter is not clear. However, the F-corona is believed to be basically stable in nature, and does not show the cycle variation (Morgan and Habbal, 2007). If this is true, the scatter is caused by the error of the brightness estimation of the F-corona due to the error in the calibration or error in the separation of the K-corona and the F-corona. Our observations were carried out during the deep solar minimum when the brightness of the K-corona is very low, and they were carefully calibrated. Therefore, our measurement of the K + F-corona gives a more accurate upper limit of the brightness of the F-corona in visible wavelengths.

5. Summary

We obtained well-calibrated brightness distributions of the white light corona in the 2008 and 2009 eclipses, when the solar activity was the lowest in one hundred years. The corona shows quite low brightness in both eclipses. In their inner part the obtained images show the coronal electron column density distribution down to just above the limb during the very low solar activity. In the outer area beyond about $3 R_{\odot}$ they show the upper limit of the F-corona in visible wavelengths, which is lower than the brightness of the F-corona in some of the previous measurements. Such modern, high-accuracy measurements of the coronal brightness in coming eclipses will reveal a more reliable relation between the solar activity and the total amount of the coronal matter.

Acknowledgements One of the authors (YH) had appealed to the participants of commercial eclipse tours to take scientific data at the eclipse in 2009. He thanks all the people who responded to the appeal and expressed their intention to try to take the data, though not all of them succeeded in the observation, and he is also grateful to E. Hiei, who helped and encouraged the collaboration. He expresses thanks also to members of the eclipse expeditions of Kagoshima University and Kyoto University, and the detachments to China and Japan's Tokara Island of the expeditions from the National Astronomical Observatory of Japan. Some of the instruments for the observation were prepared by the Advanced Technology Center at NAOJ.

References

- Druckmüller, M., Rušin, V., Minarovjech, M.: 2006, *Contrib. Astron. Obs. Skaln. Pleso* **36**, 131.
- Dürst, J.: 1982, *Astron. Astrophys.* **112**, 241.
- Fainshtein, V.G., Tsivileva, D.M., Kashapova, L.K.: 2010, *Solar Phys.* **267**, 203.
- Habbal, S.R., Druckmüller, M., Morgan, H., Daw, A., Johnson, J., Ding, A., Arndt, M., Esser, R., Rušin, V., Scholl, I.: 2010, *Astrophys. J.* **708**, 1650.
- Høg, E., Fabricius, C., Makarov, V.V., Urban, S., Corbin, T., Wycoff, G., Bastian, U., Schwekendiek, P., Wicenc, A.: 2000, *Astron. Astrophys.* **355**, L27.
- Koutchmy, S., Lamy, P.L.: 1985, In: Giese, R.H., Lamy, P. (eds.) *Properties and Interactions of Interplanetary Dust*, *IAU Colloq.* **85**, 63.
- Lebecq, C., Koutchmy, S., Stellmacher, G.: 1985, *Astron. Astrophys.* **152**, 157.
- Morgan, H., Habbal, S.R.: 2007, *Astron. Astrophys.* **471**, L47.
- Pasachoff, J.M., Rušin, V., Druckmüller, M., Aniol, P., Saniga, M., Minarovjech, M.: 2009, *Astrophys. J.* **702**, 1297.
- Pasachoff, J.M., Rušin, V., Saniga, M., Druckmüllerová, H., Babcock, B.A.: 2011, *Astrophys. J.* **742**, 29.
- Rušin, V.: 2000, In: Livingston, W., Özgüç, A. (eds.) *Last Total Solar Eclipse of the Millennium*, *ASP Conf. Ser.* **205**, 17.
- Saito, K.: 1970, *Ann. Tokyo Astron. Obs.* **12**, 53.
- Sigernes, F., Dyrland, M., Peters, N., Lorentzen, D.A., Svenøe, T., Heia, K., Chernouss, S., Deehr, Charles S., Kosch, M.: 2009, *Opt. Express* **17**, 20211.
- Skomorovsky, V.I., Trifonov, V.D., Mashnich, G.P., Zagaynova, Y.S., Fainshtein, V.G., Kushtal, G.I., Chuprakov, S.A.: 2012, *Solar Phys.* **277**, 267.
- Voulgaris, A., Athanasiadis, T., Seiradakis, J.H., Pasachoff, J.M.: 2010, *Solar Phys.* **264**, 45.